

Article

# Single-Photon Superradiance and Subradiance as Collective Emission from Symmetric and Anti-Symmetric States

Nicola Piovella<sup>1,2,\*</sup>  and Stefano Olivares<sup>1,2</sup> 

<sup>1</sup> Dipartimento di Fisica “Aldo Pontremoli”, Università degli Studi di Milano, Via Celoria 16, 20133 Milano, Italy; stefano.olivares@unimi.it

<sup>2</sup> INFN Sezione di Milano, Via Celoria 16, 20133 Milano, Italy

\* Correspondence: nicola.piovella@unimi.it

**Abstract:** Recent works have shown that collective single-photon spontaneous emission from an ensemble of  $N$  resonant two-level atoms is a rich field of study. Superradiance describes the emission from a completely symmetric state of  $N$  atoms, with a single excited atom prepared with a given phase, for instance, imprinted by an external laser. Instead, subradiance is associated with the emission from the remaining  $N - 1$  asymmetric states, with a collective decay rate less than the single-atom value. Here, we discuss the properties of the orthonormal basis of symmetric and asymmetric states and the entanglement properties of superradiant and subradiant states. On the one hand, by separating the symmetric superradiant state from the subradiant ones, we are able to determine the subradiant fraction induced in the system by the laser. On the other hand, we show that, as the external laser is switched off and the atomic excitation decays, entanglement in the atomic ensemble appears when the superradiant fraction falls below the threshold  $1/N$ .

**Keywords:** collective scattering; cold atoms; superradiance; subradiance



**Citation:** Piovella, N.; Olivares, S. Single-Photon Superradiance and Subradiance as Collective Emission from Symmetric and Anti-Symmetric States. *Symmetry* **2023**, *15*, 1817. <https://doi.org/10.3390/sym15101817>

Academic Editors: Hong Guo and Valeriy Sbitnev

Received: 26 July 2023

Revised: 15 September 2023

Accepted: 22 September 2023

Published: 25 September 2023



**Copyright:** © 2023 by the authors. Licensee MDPI, Basel, Switzerland. This article is an open access article distributed under the terms and conditions of the Creative Commons Attribution (CC BY) license (<https://creativecommons.org/licenses/by/4.0/>).

## 1. Introduction

Cooperative light scattering by a system of  $N$  two-level atoms has been a topic studied since many years [1]. Many studies in the past have been focused on a diffusive regime dominated by multiple scattering [2], where light travels over distances much larger than the mean free path. More recently, it has been shown that light scattering in dilute systems induces a dipole–dipole interaction between atom pairs, leading to a different regime dominated by single scattering of photons by many atoms. The transition between single and multiple scattering is controlled by the optical thickness parameter  $b(\Delta) = b_0 / (1 + 4\Delta^2 / \Gamma^2)$  [3,4], where  $b_0$  is the resonant optical thickness,  $\Delta$  is the detuning of the laser frequency from the atomic resonance frequency and  $\Gamma$  is the single atom decay rate. A different cooperative emission is provided by superradiance and subradiance, both originally predicted by Dicke in 1954 [5] in fully inverted system. Whereas Dicke superradiance originates from constructive interference between many emitted photons, subradiance is based on destructive interference effect, leading to the partial trapping of light. Subradiant states are important in quantum information to protect entanglement against decoherence, especially in the case of two two-level atoms forming a dark state [6,7].

Dicke states have been considered for a collection of  $N$  two-level systems [8], realized, e.g., by atoms [9] or quantum dots [10]. In contrast to an initially fully inverted system with  $N$  photons stored by  $N$  atoms, states with at most one single excitation have attracted considerable attention in the context of quantum information [11–13], where the accessible Hilbert space can be restricted to a single excitation by using, e.g., the Rydberg blockade [14–16]. A particular kind of single-excitation superradiance has been proposed by Scully and coworkers [17–19] in a system of  $N$  two-level atoms prepared by the absorption of a single photon (Timed Dicke state). A link between this single-photon superradiance and the more classical process of cooperative scattering of an incident laser

by  $N$  atoms has been proposed by a series of theoretical and experimental papers [20–22]. In such systems of driven cold atoms, subradiance has been also predicted [23] and then observed [24]; after that, the laser is abruptly switched off and the emitted photons detected in a given direction. Subradiance, by itself, has attracted a large interest for its application in quantum optics as a possible method to control spontaneous emission, storing the excitation for a relatively long time. For instance, it has been shown [25] that it is possible to use subradiance to store a photon in a small volume for many atomic lifetimes and later switch the subradiant state to a superradiant state which emits a photon in a time shorter than the single-atom lifetime. Such a process has potential applications in quantum technology, e.g., quantum memories. Furthermore, it has been proven that the distribution of the atoms in an extended ensemble has a substantial effect on cooperative spontaneous emission [26]. For instance, for atomic distributions with mirror symmetry [27], the anti-symmetric states are subradiant, even when half of the atoms are randomly distributed as long as the mirror symmetry is maintained. Periodic distribution with intrinsic mirror symmetry can be realized in ion traps, and the subradiant states can be prepared by specially tailored antisymmetric optical modes. Also, the presence of an optical cavity may enhance the generation of subradiant states. In ref. [28], it was shown that by tuning the cavity decay parameter, the nonequilibrium phase transition of cooperative resonance fluorescence changes drastically, amplifying the subradiant Dicke states through cavity-assisted coherences. Letting the system relax into the ground state generates a dark state cascade that can be utilized to store quantum information.

The aim of this paper is to provide a mathematical description of the single-excitation states in terms of superradiant and subradiant states, i.e., separating the fully symmetric state by the remaining antisymmetric ones. Symmetric and subradiant excited states are distinguished by their decay rates, once populated by a classical external laser and observed; after that, the laser is switched off: the symmetric state has a superradiant decay rate proportional to  $N\Gamma$ , where  $\Gamma$  is the single-atom decay, whereas the antisymmetric states have a decay rate slower than  $\Gamma$ .

A crucial point is to determine if such subradiant states are entangled or not, in view of a possible application as quantum memories. Once the time evolution of these states is characterized, we will apply the criteria of the spin-squeezing inequalities introduced by Tóth [29] to detect entanglement in the superradiant and subradiant states. We outline that we limit our study to the linear regime, where the excitation amplitude is proportional to the driving incident electric field. In this linear regime, we must consider the entanglement criteria which are independent from the value of the driving field, i.e., abandoning these criteria which lead to expressions which depend nonlinearly on the driving field, as will be discussed in the following.

The paper is organized as follows. In Section 2, we present the Hamiltonian describing the dynamics of  $N$  two-level atoms interacting with the driving field and write the equation of motion in the linear regime. Then, we calculate the decay rate and the transition rates between different elements of the so-called Timed Dicke basis with its symmetric and antisymmetric states. Section 3 introduces the collective spin operator and the formalism of the spin-squeezing inequalities to assess entanglement. Conclusions are eventually drawn in Section 4.

## 2. The Model

We consider  $N \gg 1$  two-level atoms with the same atomic transition frequency  $\omega_a$ , linewidth  $\Gamma$  and dipole  $d$  (polarization effects are neglected). The atoms are driven by a monochromatic plane wave with electric field  $E_0$ , frequency  $\omega_0$  and wave vector  $\mathbf{k}_0$ , detuned from the atomic transition by  $\Delta_0 = \omega_0 - \omega_a$  (see Figure 1);  $|g_j\rangle$  and  $|e_j\rangle$  are the ground and excited states, respectively, of the  $j$ -th atom,  $j = 1, \dots, N$ , which is placed at position  $\mathbf{r}_j$ .

We consider the single excitation effective Hamiltonian [30,31] in the scalar approximation. This approximation is appropriate in the dilute limit, where inter-atomic distances

are larger than the optical wavelength, making near-field terms decaying as  $1/r^3$  negligible. If we assume that only one photon is present, when tracing over the radiation degrees of freedom, the dynamics of the atomic system can be described by the non-Hermitian Hamiltonian  $\hat{H} = \hat{H}_0 - i\hat{H}_{\text{eff}}$ , where [30,32]

$$\hat{H}_0 = -\hbar\Delta_0 \sum_{j=1}^N \hat{\sigma}_j^\dagger \hat{\sigma}_j + \frac{\hbar\Omega_0}{2} \sum_{j=1}^N \left( \hat{\sigma}_j e^{-i\mathbf{k}_0 \cdot \mathbf{r}_j} + \hat{\sigma}_j^\dagger e^{i\mathbf{k}_0 \cdot \mathbf{r}_j} \right) \quad (1)$$

$$\hat{H}_{\text{eff}} = \frac{\hbar\Gamma}{2} \sum_{j,m} G_{jm} \hat{\sigma}_j^\dagger \hat{\sigma}_m. \quad (2)$$

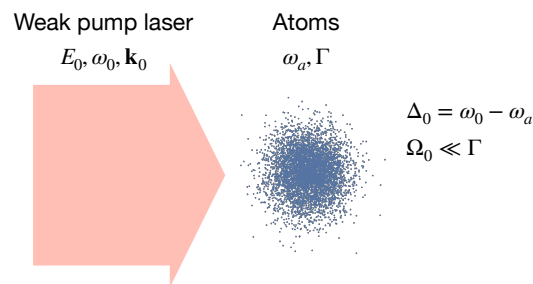


**Figure 1.** Scheme of the system and parameters.

Here,  $\Omega_0 = dE_0/\hbar$  is the Rabi frequency,  $\hat{\sigma}_j = |g_j\rangle\langle e_j|$  and  $\hat{\sigma}_j^\dagger = |e_j\rangle\langle g_j|$  are the lowering and raising operators, with commutations rules  $[\hat{\sigma}_j, \hat{\sigma}_m^\dagger] = -\delta_{jm}\hat{\sigma}_{zj}$ , where  $\hat{\sigma}_{zj} = |e_j\rangle\langle e_j| - |g_j\rangle\langle g_j|$  are the population difference operators, and

$$G_{jm} = \begin{cases} \Gamma_{jm} - i\Omega_{jm} & \text{if } j \neq m, \\ 1 & \text{if } j = m, \end{cases} \quad (3)$$

where

$$\Gamma_{jm} = \frac{\sin(k_0 r_{jm})}{k_0 r_{jm}} \quad \text{and} \quad \Omega_{jm} = \frac{\cos(k_0 r_{jm})}{k_0 r_{jm}}. \quad (4)$$

Note that  $\hat{H}_{\text{eff}}$  contains both real and imaginary parts, which takes into account that the excitation is not conserved since it can leave the system by emission. By writing the Heisenberg's equations for the operators  $\hat{\sigma}_j$  and  $\hat{\sigma}_{zj}$ , one can solve them by iteration in powers of  $\Omega_0$ . One can see that assuming weak excitation ( $\Omega_0 \ll \Gamma$ ), we can approximate (in the Heisenberg's equation for  $\hat{\sigma}_j$ )  $\hat{\sigma}_{zj} \approx \hat{I}_j$ , where  $\hat{I}_j$  is the identity operator for the  $j$ th atom [33]. Following the approach reported in refs. [30–32], one can show that this approximation amounts to the linear regime in which all the processes generating more than one photon at the same time are neglected [33]. Thereafter, only one atom among the  $N$  atoms can be found in the excited state, whereas all others are in their ground state. Then, the generic state of the atomic system belongs to an  $(N + 1)$ -dimensional Hilbert space and can be written as [17,25]

$$|\Psi\rangle = \alpha|g\rangle + \sum_{j=1}^N \beta_j e^{i\mathbf{k}_0 \cdot \mathbf{r}_j} |j\rangle \quad (5)$$

where  $|g\rangle = |g_1, \dots, g_N\rangle$  and  $|j\rangle = |g_1, \dots, e_j, \dots, g_N\rangle$ ,  $j = 1, \dots, N$ . From the Schrödinger equation  $i\hbar(\partial/\partial t)|\Psi\rangle = \hat{H}|\Psi\rangle$  and assuming  $\alpha \approx 1$  in the weak-excitation approximation, we obtain the following equations for the coefficients  $\beta_j$  of the state (5):

$$\dot{\beta}_j = \left( i\Delta_0 - \frac{\Gamma}{2} \right) \beta_j - \frac{i\Omega_0}{2} - \frac{\Gamma}{2} \sum_{m \neq j} \tilde{G}_{jm} \beta_m(t), \quad (j = 1, \dots, N) \quad (6)$$

where  $\dot{\beta}_j$  refers to the time derivative of the coefficient  $\beta_j$  and  $\tilde{G}_{jm} = G_{jm}e^{-i\mathbf{k}_0 \cdot (\mathbf{r}_j - \mathbf{r}_m)}$ . We observe that a more fundamental Master equation approach, describing the atomic system dynamics within the same approximations (scalar approximation and single-excitation approximation), leads to the same Equation (6) [22,32].

The use of the bare basis  $\{|g\rangle, |j\rangle\}$  has the advantage that Equation (6) can be easily solved numerically. However, it does not distinguish between symmetric and anti-symmetric states that play a relevant role in our investigation. For this reason we introduce the Timed Dicke (TD) basis with a single excitation [18,34]:

$$\{|g\rangle, |+\rangle_{\mathbf{k}_0}, |1\rangle_{\mathbf{k}_0}, \dots, |N-1\rangle_{\mathbf{k}_0}\}, \tag{7}$$

where  $|g\rangle$  has been introduced above, whereas

$$|+\rangle_{\mathbf{k}_0} = \frac{1}{\sqrt{N}} \sum_{j=1}^N e^{i\mathbf{k}_0 \cdot \mathbf{r}_j} |j\rangle \tag{8}$$

is the symmetric Timed Dicke (STD) state and

$$|s\rangle_{\mathbf{k}_0} = \frac{1}{\sqrt{s(s+1)}} \left\{ \sum_{j=1}^s e^{i\mathbf{k}_0 \cdot \mathbf{r}_j} |j\rangle - s e^{i\mathbf{k}_0 \cdot \mathbf{r}_{s+1}} |s+1\rangle \right\}, \quad (s = 1, \dots, N-1) \tag{9}$$

are the anti-symmetric ones. The advantage of using the TD basis is that  $|s\rangle_{\mathbf{k}_0}$  are collective states involving  $s + 1$  atoms. Considering (9) and the definition of  $|+\rangle_{\mathbf{k}_0}$ , it is straightforward to verify that, within the considered Hilbert space, the TD basis is complete, namely:

$$|g\rangle\langle g| + |+\rangle_{\mathbf{k}_0}\langle +| + \sum_{s=1}^{N-1} |s\rangle_{\mathbf{k}_0}\langle s| = \hat{I} \tag{10}$$

and orthonormal, since  $\langle g|+\rangle_{\mathbf{k}_0} = \langle g|s\rangle_{\mathbf{k}_0} = \langle \mathbf{k}_0|+\rangle_{\mathbf{k}_0} = 0$ , and  $\langle \mathbf{k}_0|s\rangle_{\mathbf{k}_0} = \delta_{s,s'}$ .

To highlight the physical meaning of the TD states, it is useful to evaluate the following transition rates between the basis elements. On the one hand, we find

$$\langle \mathbf{k}_0|+\rangle_{\mathbf{k}_0} \langle \hat{H}_0|+\rangle_{\mathbf{k}_0} = -\hbar\Delta_0 \quad \text{and} \quad \langle \mathbf{k}_0|+\rangle_{\mathbf{k}_0} \langle \hat{H}_{\text{eff}}|+\rangle_{\mathbf{k}_0} = \frac{\hbar\Gamma_+}{2} - i\hbar\Omega_+ \tag{11}$$

with  $\hat{H}_0$  and  $\hat{H}_{\text{eff}}$  given in Equations (1) and (2), respectively, and

$$\Gamma_+ = \Gamma \left( 1 + \frac{1}{N} \sum_{j=1}^N \sum_{\substack{m=1 \\ (m \neq j)}}^N \tilde{\Gamma}_{jm} \right), \tag{12}$$

$$\Omega_+ = \frac{\Gamma}{N} \sum_{j=1}^N \sum_{\substack{m=1 \\ (m \neq j)}}^N \tilde{\Omega}_{jm} \tag{13}$$

where

$$\tilde{\Gamma}_{jm} = \Gamma_{jm} \cos[\mathbf{k}_0 \cdot (\mathbf{r}_j - \mathbf{r}_m)] \quad \text{and} \quad \tilde{\Omega}_{jm} = \Omega_{jm} \cos[\mathbf{k}_0 \cdot (\mathbf{r}_j - \mathbf{r}_m)] \tag{14}$$

and  $\Gamma_{jm}$  and  $\Omega_{jm}$  have been introduced in Equation (4). For a cloud of cold atoms with a Gaussian distribution with parameter  $\sigma_r$ , one can prove that  $\Gamma_+ \approx \Gamma(1 + b_0/12)$  [21,33], where  $b_0 = 3N/\sigma^2$  is the resonant optical thickness, with  $\sigma = k_0\sigma_r$ . Thus, we can conclude that  $|+\rangle_{\mathbf{k}_0}$  is a *superradiant* state for very large  $b_0$  [18,19].

On the other hand, the transition rates for the states  $|s\rangle_{\mathbf{k}_0}$ ,  $s = 1, \dots, N-1$ , read

$$\langle \mathbf{k}_0|s\rangle_{\mathbf{k}_0} \langle \hat{H}_0|s\rangle_{\mathbf{k}_0} = -\hbar\Delta_0 \quad \text{and} \quad \langle \mathbf{k}_0|s\rangle_{\mathbf{k}_0} \langle \hat{H}_{\text{eff}}|s\rangle_{\mathbf{k}_0} = \frac{\hbar\Gamma_s}{2} - i\hbar\Omega_s \tag{15}$$

with

$$\Gamma_s = \Gamma \left[ 1 + \frac{1}{s+1} \left( \frac{1}{s} \sum_{j=1}^s \sum_{\substack{m=1 \\ (m \neq j)}}^s \tilde{\Gamma}_{jm} - 2 \sum_{j=1}^s \tilde{\Gamma}_{j,s+1} \right) \right], \tag{16}$$

$$\Omega_s = \frac{\Gamma}{2(s+1)} \left( \frac{1}{s} \sum_{j \neq m=1}^s \tilde{\Omega}_{jm} - 2 \sum_{j=1}^s \tilde{\Omega}_{j,s+1} \right). \tag{17}$$

In this case, the decay rates  $\Gamma_s$  are less than the single-atom decay rate  $\Gamma$ , and the states  $|s\rangle_{\mathbf{k}_0}$  turn out to be *subradiant* [25].

Now we focus on the state (5), which, in the TD basis, reads

$$|\Psi\rangle = \alpha |g\rangle + \beta_+ |+\rangle_{\mathbf{k}_0} + \sum_{s=1}^{N-1} \gamma_s |s\rangle_{\mathbf{k}_0}, \tag{18}$$

with

$$\beta_+ = {}_{\mathbf{k}_0} \langle + | \Psi \rangle = \frac{1}{\sqrt{N}} \sum_{j=1}^N \beta_j, \tag{19}$$

$$\gamma_s = {}_{\mathbf{k}_0} \langle s | \Psi \rangle = \frac{1}{\sqrt{s(s+1)}} \left( \sum_{j=1}^s \beta_j - s \beta_{s+1} \right). \tag{20}$$

Thanks to the considerations made above about the properties of the TD states, we can easily find the probability to find our state in a superradiant, i.e., STD, and subradiant state, that is:

$$P_+ = |\beta_+|^2 \tag{21}$$

and

$$P_{\text{sub}} = \sum_{s=1}^{N-1} |\gamma_s|^2, \tag{22}$$

respectively. Moreover, from the normalization of the state  $|\Psi\rangle$ , it follows that

$$\sum_{j=1}^N |\beta_j|^2 = |\beta_+|^2 + \sum_{s=1}^{N-1} |\gamma_s|^2 = P_+ + P_{\text{sub}}. \tag{23}$$

Finally, the superradiant fraction of excited atoms is given by

$$f_{\text{SR}} = \frac{P_+}{P_+ + P_{\text{sub}}} = \frac{|\bar{\beta}|^2}{|\beta|^2} \tag{24}$$

where we introduced the mean quantities:

$$|\bar{\beta}|^2 = \frac{1}{N} \sum_{j=1}^N |\beta_j|^2 \tag{25}$$

$$|\beta| = \frac{1}{N} \left| \sum_{j=1}^N \beta_j \right|. \tag{26}$$

In turn, the subradiant fraction is  $f_{\text{sub}} = 1 - f_{\text{SR}}$ .

### 3. Entanglement Properties of the Superradiant and Subradiant Collective States

As the system we are investigating in this paper consists of a large number of atoms,  $N \gg 1$ , we cannot assess its entanglement properties by individually addressing the single

particles. Nevertheless, it is known that spin-squeezing can be used to create large-scale entanglement [35]. A two-level atom can be considered a spin-1/2 system, described in terms of Pauli’s operators of the angular moments. Therefore, here we consider suitable generalized spin-squeezing inequalities [29] based only on collective quantities that are accessible and can be measured experimentally.

Given  $N$  two-level atoms, we start defining the following collective angular momentum operators:

$$\hat{J}_k = \frac{1}{2} \sum_{j=1}^N \hat{\sigma}_j^{(k)}, \quad (k = x, y, z) \tag{27}$$

where  $\hat{\sigma}_j^{(k)}$  are the Pauli matrices associated with the  $j$ -th atom. If we assume the state given by Equation (5), we can calculate the expectation values of the first and second moments of  $\hat{J}_k$  using the result of the previous section (see Appendix A for details):

$$\langle \hat{J}_x \rangle = \Re[\alpha^* \sum_{j=1}^N \beta_j], \tag{28}$$

$$\langle \hat{J}_y \rangle = -\Im[\alpha^* \sum_{j=1}^N \beta_j], \tag{29}$$

$$\langle \hat{J}_z \rangle = -N \left( \frac{1}{2} - |\bar{\beta}|^2 \right), \tag{30}$$

and

$$\langle \hat{J}_x^2 \rangle = \langle \hat{J}_y^2 \rangle = \frac{N}{2} \left( \frac{1}{2} + N |\bar{\beta}|^2 - |\bar{\beta}|^2 \right), \tag{31}$$

$$\langle \hat{J}_z^2 \rangle = N \left[ \frac{N}{4} - (N - 1) |\bar{\beta}|^2 \right], \tag{32}$$

$\beta_j$  being the solutions of Equation (6) and  $|\bar{\beta}|^2$  and  $|\bar{\beta}|$  are given in Equations (25) and (26), respectively. One can also straightforwardly evaluate the corresponding variances  $(\Delta \hat{J}_k)^2 = \langle \hat{J}_k^2 \rangle - \langle \hat{J}_k \rangle^2, k = x, y, z$ .

In ref. [29], G. Tóth and co-workers proved that a sufficient condition to have entanglement is the violation of suitable inequalities involving the first and second moments of the  $\hat{J}_k$  operators evaluated above. Though they proposed four inequalities, in our case, only one of them is relevant to our system, namely:

$$(\Delta \hat{J}_x)^2 + (\Delta \hat{J}_y)^2 + (\Delta \hat{J}_z)^2 \geq \frac{N}{2}, \tag{33}$$

since the other three Tóth’s inequalities in ref. [29] are:

$$\langle \hat{J}_x^2 \rangle + \langle \hat{J}_y^2 \rangle + \langle \hat{J}_z^2 \rangle \leq \frac{N(N + 2)}{4}, \tag{34a}$$

$$\langle \hat{J}_k^2 \rangle + \langle \hat{J}_l^2 \rangle - \frac{N}{2} \leq (N - 1)(\Delta \hat{J}_m)^2, \tag{34b}$$

$$(N - 1) \left[ (\Delta \hat{J}_k)^2 + (\Delta \hat{J}_l)^2 \right] \geq \langle \hat{J}_m^2 \rangle + \frac{N(N - 2)}{4} \tag{34c}$$

(where  $k, l, m$  take all the possible permutations of  $x, y, z$ ) are not useful, as the first and the third are never violated, whereas the second one leads to a condition on the  $\beta_j$  going beyond the linear regime assumed to solve Equation (6), as shown in Appendix B.

The inequality (33) is more interesting. Its l.h.s. can be rewritten as a function of the superradiant fraction (24), that is:

$$(\Delta \hat{J}_x)^2 + (\Delta \hat{J}_y)^2 + (\Delta \hat{J}_z)^2 = \frac{N}{2} + N^2 \overline{|\beta|^2} \left( N \overline{|\beta|^2} - \overline{|\beta|^2} \right) \quad (35)$$

$$= \frac{N}{2} + N^2 \left( \overline{|\beta|^2} \right)^2 (N f_{SR} - 1), \quad (36)$$

which can be solved within the linear regime assumed throughout the paper. Hence, the inequality (33) is violated when the superradiant fraction is  $f_{SR} < 1/N$ , thus highlighting the entanglement of the collective atomic state. This will occur when the driving laser is cut and the superradiant component decays faster than the subradiant one, until the subradiant fraction becomes larger than  $1 - 1/N$ .

Figures 2–4 present a typical result. We numerically evaluate the values of  $\beta_j$  solving the linear Equation (6) for  $N = 10^3$  and a Gaussian distribution with  $\sigma = k_0 \sigma_r = 10$ . The laser is cut off after  $\Gamma t = 20$ . Figure 2 shows  $P = (1/N) \sum_j |\beta_j|^2$  for  $\Delta_0 = 10\Gamma$  vs. time. Figure 3 shows the left-hand side of Equation (33) normalized to  $N$ , i.e.,  $C = [(\Delta \hat{J}_x)^2 + (\Delta \hat{J}_y)^2 + (\Delta \hat{J}_z)^2]/N$  vs. time, for the same parameters of Figure 2 and three different values of detuning,  $\Delta_0 = 8\Gamma$  (red line),  $\Delta_0 = 9\Gamma$  (blue line) and  $\Delta_0 = 10\Gamma$  (black line). The inset shows the region where the inequality (33) is violated, namely when  $C < 1/2$ . Figure 4 shows the superradiant and subradiant fractions,  $f_{SR}$  (continuous blue line) and  $f_{sub}$  (dashed red line), as defined by Equation (24), for the same parameters of Figure 2. The dotted black line is the value  $1/N$ . We observe that when the laser is on, the subradiant fraction is only about the 3% of the total excitation. As soon as the laser is cut off, the superradiant fraction decays fast and the subradiant fraction increases, becoming dominating for  $\Gamma t > 20.5$ . The atoms become entangled when  $f_{SR} < 1/N$ , at time larger than  $\Gamma t > 24$ .

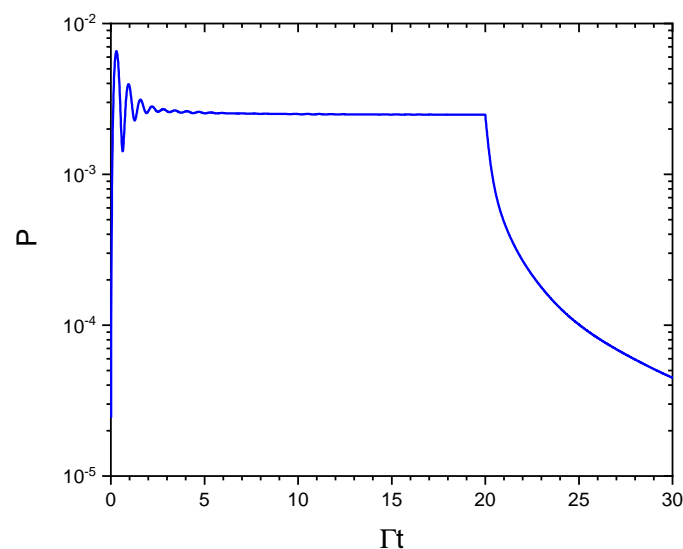


**Figure 2.** Plot of  $P = (1/N) \sum_j |\beta_j|^2$  vs. time, obtained by solving Equation (6) for  $N = 10^3$ ,  $\Delta_0 = 10\Gamma$  and a Gaussian distribution with  $\sigma = k_0 \sigma_R = 10$ . The laser is cut off after  $\Gamma t = 20$ .

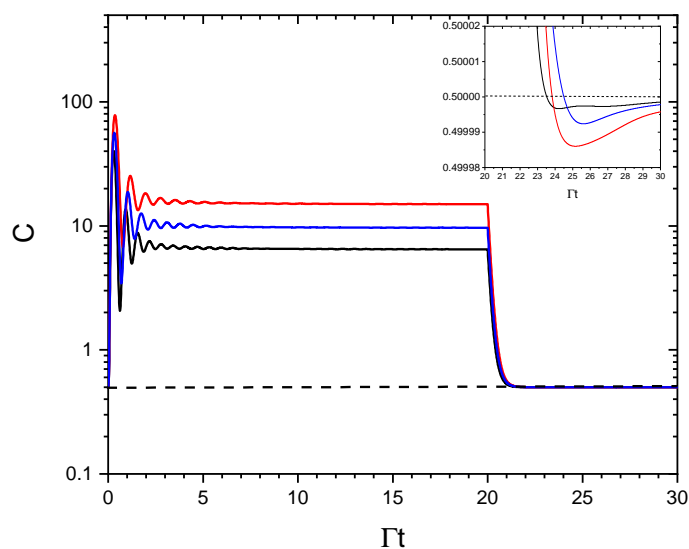


**Figure 3.**  $C = [(\Delta \hat{f}_x)^2 + (\Delta \hat{f}_y)^2 + (\Delta \hat{f}_z)^2]/N$  vs. time for the same parameters of Figure 2 and three different values of detuning,  $\Delta_0 = 8\Gamma$  (red line),  $\Delta_0 = 9\Gamma$  (blue line) and  $\Delta_0 = 10\Gamma$  (black line). The inset magnifies the plot around  $C = 1/2$ , showing the violation of the spin-squeezing inequality (33).

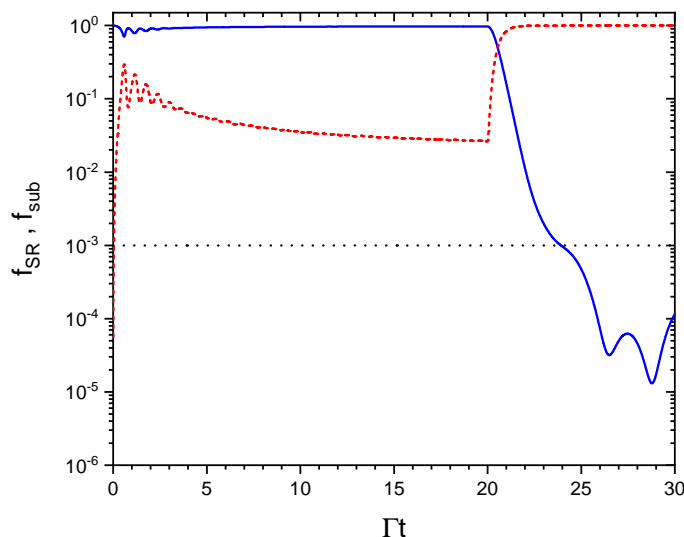


**Figure 4.** Superradiant and subradiant fractions,  $f_{SR}$  (continuous blue line) and  $f_{sub}$  (dashed red line), for the same parameters of Figure 2. The dotted black line is the value  $1/N$ .

#### 4. Conclusions

In this work, we addressed the open question concerning the relation between the entanglement of an atomic ensemble and its superradiant and subradiant fraction. To this aim, we considered the state of  $N$  two-level atoms with positions  $\mathbf{r}_j$  (with  $j = 1, \dots, N$ ), where only one is excited among them. Then, we discussed their symmetry properties: the single-excitation Hilbert space can be spanned by a completely symmetric state (the “Symmetric Timed Dicke state”) and  $N - 1$  asymmetric ones, where the first has a superradiant decay rate proportional to  $N$ , while the others have subradiant decay rates less than the single-atom value. Remarkably, the projection on the symmetric and asymmetric states allows us to calculate the superradiant and subradiant fractions of the ensemble.

To address the problem of the birth of the entanglement, we studied the relevant case of an ensemble of  $N$  atoms driven by an external, uniform laser. In the framework of the linear regime, the probability amplitude of excitation is proportional to the incident electric field, and the superradiant fraction is largely dominant, with only a small fraction of atoms in the subradiant states. However, when the laser is cut off, the superradiant

fraction rapidly decays to zero, leaving only the superradiant one, as it has been observed in the experiments of ref. [24].

In order to investigate the entanglement properties of the atomic ensemble, we exploited suitable spin squeezing inequalities, based on the first and the second order moments of collective spin operators. We have found that one of these inequalities is violated when the superradiant fraction decreases below the value  $1/N$ . Therefore, to have entanglement the probability of finding  $N$  atoms in the superradiant state must be less than the average probability per atom to be in the excited state. Conversely, when the superradiant fraction is larger than  $1/N$ , no entanglement can be detected by measuring the moments of the collective spin operators.

**Author Contributions:** All authors conceived the study and contributed to writing of the manuscript. All authors have read and agreed to the published version of the manuscript.

**Funding:** This research received no external funding.

**Data Availability Statement:** Not applicable.

**Conflicts of Interest:** The authors declare no conflict of interest.

### Appendix A. Calculation of the First and Second Moments of $\hat{J}_k$

In this appendix, we explicitly calculate the first and second moments of the collective angular momentum operators used in the text, namely:

$$\hat{J}_k = \frac{1}{2} \sum_{j=1}^N \hat{\sigma}_j^{(k)}, \quad (k = x, y, z) \quad (\text{A1})$$

where  $\hat{\sigma}_j^{(k)}$  are the Pauli matrices associated with the  $j$ -th atom. It is useful to introduce the identities  $\hat{\sigma}_j^\dagger = (\hat{\sigma}_j^{(x)} + i\hat{\sigma}_j^{(y)})/2$  and  $\hat{\sigma}_j = (\hat{\sigma}_j^{(x)} - i\hat{\sigma}_j^{(y)})/2$ , which are the raising and lowering operators appearing in Equations (1) and (2), and  $\sigma_j^{(z)} = |e_j\rangle\langle e_j| - |g_j\rangle\langle g_j|$ . We define

$$\tilde{\sigma}_j^\dagger = e^{i\mathbf{k}_0 \cdot \mathbf{r}_j} \hat{\sigma}_j^\dagger, \quad \tilde{\sigma}_j = e^{-i\mathbf{k}_0 \cdot \mathbf{r}_j} \hat{\sigma}_j \quad (\text{A2})$$

and the collective operators:

$$\hat{J}_- = \sum_{j=1}^N \tilde{\sigma}_j, \quad \hat{J}_+ = \sum_{j=1}^N \tilde{\sigma}_j^\dagger \quad \text{and} \quad \hat{J}_z = \frac{1}{2} \sum_{j=1}^N \hat{\sigma}_j^{(z)} \quad (\text{A3})$$

with commutation relations:

$$[\hat{J}_+, \hat{J}_-] = 2\hat{J}_z, \quad [\hat{J}_z, \hat{J}_\pm] = \pm 2\hat{J}_\pm. \quad (\text{A4})$$

We can now apply the formalism of ref. [29], calculating the first- and second-order moments of the collective operators  $\hat{J}_x = (\hat{J}_+ + \hat{J}_-)/2$  and  $\hat{J}_y = (\hat{J}_+ - \hat{J}_-)/(2i)$ . Explicitly,

$$\langle \hat{J}_x \rangle = \frac{1}{2} \{ \langle \hat{J}_+ \rangle + \langle \hat{J}_- \rangle \}, \quad (\text{A5})$$

$$\langle \hat{J}_y \rangle = \frac{1}{2i} \{ \langle \hat{J}_+ \rangle - \langle \hat{J}_- \rangle \}, \quad (\text{A6})$$

$$\langle \hat{J}_x^2 \rangle = \frac{1}{4} \{ \langle \hat{J}_+ \hat{J}_- \rangle + \langle \hat{J}_- \hat{J}_+ \rangle + \langle \hat{J}_+^2 \rangle + \langle \hat{J}_-^2 \rangle \}, \quad (\text{A7})$$

$$\langle \hat{J}_y^2 \rangle = \frac{1}{4} \{ \langle \hat{J}_+ \hat{J}_- \rangle + \langle \hat{J}_- \hat{J}_+ \rangle - \langle \hat{J}_+^2 \rangle - \langle \hat{J}_-^2 \rangle \}, \quad (\text{A8})$$

where the expectations are evaluated using the  $\beta_j$  as evaluated from Equation (6) (see Section 2). Since

$$\tilde{\sigma}_j|\Psi\rangle = \beta_j|g\rangle, \quad (\text{A9})$$

$$\tilde{\sigma}_j^\dagger|\Psi\rangle = \alpha e^{i\mathbf{k}_0 \cdot \mathbf{r}_j}|j\rangle, \quad (\text{A10})$$

$$\begin{aligned} \hat{\sigma}_j^{(z)}|\Psi\rangle &= -\alpha|g\rangle + \beta_j e^{i\mathbf{k}_0 \cdot \mathbf{r}_j}|j\rangle - \sum_{m=1}^N (1 - \delta_{jm})\beta_m e^{i\mathbf{k}_0 \cdot \mathbf{r}_m}|m\rangle \\ &= -|\Psi\rangle + 2\beta_j e^{i\mathbf{k}_0 \cdot \mathbf{r}_j}|j\rangle, \end{aligned} \quad (\text{A11})$$

we derive

$$\langle \hat{J}_- \rangle = \sum_{j=1}^N \langle \tilde{\sigma}_j \rangle = \alpha^* \sum_{j=1}^N \beta_j, \quad (\text{A12})$$

$$\langle \hat{J}_+ \rangle = \sum_{j=1}^N \langle \tilde{\sigma}_j^\dagger \rangle = \alpha \sum_{j=1}^N \beta_j^*, \quad (\text{A13})$$

$$\langle \hat{J}_z \rangle = \frac{1}{2} \sum_j \langle \hat{\sigma}_j^{(z)} \rangle = -\frac{N}{2} + \sum_j |\beta_j|^2, \quad (\text{A14})$$

$$\langle \hat{J}_x \rangle = \Re \left[ \alpha^* \sum_{j=1}^N \beta_j \right], \quad (\text{A15})$$

$$\langle \hat{J}_y \rangle = -\Im \left[ \alpha^* \sum_{j=1}^N \beta_j \right]. \quad (\text{A16})$$

Recalling that the system has a single excitation, we have  $\tilde{\sigma}_j \tilde{\sigma}_m^\dagger |\Psi\rangle = 0$  and  $\tilde{\sigma}_j^\dagger \tilde{\sigma}_m^\dagger |\Psi\rangle = 0$ , and we obtain:

$$\langle \hat{J}_-^2 \rangle = \langle \hat{J}_+^2 \rangle = 0. \quad (\text{A17})$$

Furthermore,

$$\begin{aligned} \langle \hat{J}_+ \hat{J}_- \rangle &= \sum_{j,m} \langle \tilde{\sigma}_j^\dagger \tilde{\sigma}_j \rangle \\ &= \sum_{j,m} \beta_j^* \beta_m = \left| \sum_{j=1}^N \beta_j \right|^2 \end{aligned} \quad (\text{A18})$$

and, using the commutation rule (A4) and Equations (A14) and (A18), we find

$$\begin{aligned} \langle \hat{J}_- \hat{J}_+ \rangle &= \langle \hat{J}_+ \hat{J}_- \rangle - 2\langle \hat{J}_z \rangle \\ &= N + \left| \sum_{j=1}^N \beta_j \right|^2 - 2 \sum_{j=1}^N |\beta_j|^2. \end{aligned} \quad (\text{A19})$$

From these results, we can calculate the expectations of  $\langle \hat{J}_k^2 \rangle$ ,  $k = x, y, z$ , namely:

$$\langle \hat{J}_x^2 \rangle = \langle \hat{J}_y^2 \rangle = \frac{N}{4} + \frac{1}{2} \left| \sum_{j=1}^N \beta_j \right|^2 - \frac{1}{2} \sum_{j=1}^N |\beta_j|^2, \quad (\text{A20})$$

$$\langle \hat{J}_z^2 \rangle = \frac{N^2}{4} - (N-1) \sum_{j=1}^N |\beta_j|^2. \quad (\text{A21})$$

It is remarkable that the second-order moments do not depend on  $\alpha$ , which appears only in the expression for  $\langle \hat{J}_{x,y} \rangle$ .

We are now ready to also evaluate the variances in the collective angular momentum operators. Defining  $(\Delta \hat{A})^2 = \langle \hat{A}^2 \rangle - \langle \hat{A} \rangle^2$ , we have:

$$(\Delta \hat{J}_x)^2 = \frac{N}{4} + \frac{1}{2} \left| \sum_{j=1}^N \beta_j \right|^2 - \frac{1}{2} \sum_{j=1}^N |\beta_j|^2 - \left\{ \Re \left[ \alpha^* \sum_{j=1}^N \beta_j \right] \right\}^2 \quad (\text{A22})$$

$$(\Delta \hat{J}_y)^2 = \frac{N}{4} + \frac{1}{2} \left| \sum_{j=1}^N \beta_j \right|^2 - \frac{1}{2} \sum_{j=1}^N |\beta_j|^2 - \left\{ \Im \left[ \alpha^* \sum_{j=1}^N \beta_j \right] \right\}^2 \quad (\text{A23})$$

$$(\Delta \hat{J}_z)^2 = \left( \sum_{j=1}^N |\beta_j|^2 \right) \left( 1 - \sum_{j=1}^N |\beta_j|^2 \right). \quad (\text{A24})$$

Notice that

$$(\Delta \hat{J}_x)^2 + (\Delta \hat{J}_y)^2 = \frac{N}{2} - \left( \sum_{j=1}^N |\beta_j|^2 \right) \left( 1 - \left| \sum_{j=1}^N \beta_j \right|^2 \right) \quad (\text{A25})$$

which is independent of  $\alpha$ .

All the previous results can be simplified by introducing the mean quantities  $\overline{|\beta|^2}$  and  $|\bar{\beta}|$  given in Equations (25) and (26), respectively. The corresponding expressions are directly reported in Section 3.

### Appendix B. Considerations on Equations (34b) and (34c)

In this appendix, we show that, in our case, Equations (34a), (34b) and (34c) cannot lead to useful conclusions.

In our case, the l.h.s. of Equation (34a) reads:

$$\langle \hat{J}_x^2 \rangle + \langle \hat{J}_y^2 \rangle + \langle \hat{J}_z^2 \rangle = \frac{N(N+2)}{4} - N^2 \sigma_\beta^2 \quad (\text{A26})$$

where we defined the particle variance as

$$\sigma_\beta^2 = \overline{|\beta|^2} - |\bar{\beta}|^2, \quad (\text{A27})$$

$$= \frac{1}{N} \sum_{s=1}^{N-1} |\gamma_s|^2. \quad (\text{A28})$$

As one may expect, Equation (34a) is true, and the equality sign holds for all the symmetric states, with  $\sigma_\beta = 0$  or, equivalently,  $f_{\text{SR}} = 1$ .

Concerning Equation (34b), if we study the following expression (similar results can be obtained for the other combination of the involved expectations):

$$\langle \hat{J}_x^2 \rangle + \langle \hat{J}_y^2 \rangle - \frac{N}{2} \leq (N-1) (\Delta \hat{J}_z)^2, \quad (\text{A29})$$

we derive:

$$|\bar{\beta}|^2 \leq \overline{|\beta|^2} [1 - (N-1) \overline{|\beta|^2}] \quad (\text{A30})$$

or, equivalently:

$$\sigma_\beta \geq \sqrt{N-1} \left( |\bar{\beta}|^2 + \sigma_\beta^2 \right). \quad (\text{A31})$$

We can clearly see that these inequalities are nonlinear in  $|\overline{\beta}|^2$ . Recalling Equations (25) and (26), we conclude that they cannot lead to useful conditions, since the solution of (A30) or (A31) depends on the  $\beta_j^2$  and thus on  $\Omega_0^2$ , whereas the  $\beta_j$  have been obtained in the framework of the linear regime with respect  $\Omega_0$ , see Equation (6).

Equation (34c) is never violated for our system. In fact, for instance, we have:

$$(N - 1)[(\Delta\hat{f}_x)^2 + (\Delta\hat{f}_y)^2] \geq \langle \hat{f}_z^2 \rangle + \frac{N(N - 2)}{4} \quad (\text{A32})$$

which, using Equations (A25) and (A21), yields

$$N^2 \overline{|\beta|^2} |\overline{\beta}|^2 > 0. \quad (\text{A33})$$

## References

- Lehmberg, R.H. Radiation from an  $N$ -Atom System. I. General Formalism. *Phys. Rev. A* **1970**, *2*, 883–888. [[CrossRef](#)]
- van der Mark, M.B.; van Albada, M.P.; Lagendijk, A. Light scattering in strongly scattering media: Multiple scattering and weak localization. *Phys. Rev. B* **1988**, *37*, 3575–3592. [[CrossRef](#)] [[PubMed](#)]
- Labeyrie, G.; Vaujour, E.; Mueller, C.A.; Delande, D.; Miniatura, C.; Wilkowski, D.; Kaiser, R. Slow diffusion of light in a cold atomic cloud. *Phys. Rev. Lett.* **2003**, *91*, 223904. [[CrossRef](#)] [[PubMed](#)]
- Guerin, W.; Rouabah, M.; Kaiser, R. Light interacting with atomic ensembles: Collective, cooperative and mesoscopic effects. *J. Mod. Opt.* **2017**, *64*, 895–907. [[CrossRef](#)]
- Dicke, R.H. Coherence in Spontaneous Radiation Processes. *Phys. Rev.* **1954**, *93*, 99–100. [[CrossRef](#)]
- Nourmandipour, A.; Vafafard, A.; Mortezapour, A.; Franzosi, R. Entanglement protection of classically driven qubits in a lossy cavity. *Sci. Rep.* **2021**, *11*, 16259. [[CrossRef](#)]
- Taghipour, J.; Mojaveri, B.; Dehghani, A. Witnessing entanglement between two two-level atoms coupled to a leaky cavity via two-photon relaxation. *Eur. Phys. J. Plus* **2022**, *137*, 772. [[CrossRef](#)]
- Mandel, L.; Wolf, E. *Optical Coherence and Quantum Optics*; Cambridge University Press: Cambridge, UK, 1995.
- Gross, M.; Haroche, S. Superradiance: An essay on the theory of collective spontaneous emission. *Phys. Rep.* **1982**, *93*, 301–396. [[CrossRef](#)]
- Lodahl, P.; Floris van Driel, A.; Nikolaev, I.S.; Irman, A.; Overgaag, K.; Vanmaekelbergh, D.; Vos, W.L. Controlling the dynamics of spontaneous emission from quantum dots by photonic crystals. *Nature* **2004**, *430*, 654–657. [[CrossRef](#)]
- Brandes, T. Coherent and collective quantum optical effects in mesoscopic systems. *Phys. Rep.* **2005**, *408*, 315–474. [[CrossRef](#)]
- Karasik, R.I.; Marzlin, K.P.; Sanders, B.C.; Whaley, K.B. Multiparticle decoherence-free subspaces in extended systems. *Phys. Rev. A* **2007**, *76*, 012331. [[CrossRef](#)]
- Pedersen, L.H.; Mølmer, K. Few qubit atom-light interfaces with collective encoding. *Phys. Rev. A* **2009**, *79*, 012320. [[CrossRef](#)]
- Tong, D.; Farooqi, S.; Stanojevic, J.; Krishnan, S.; Zhang, Y.; Côté, R.; Eyler, E.; Gould, P. Local blockade of Rydberg excitation in an ultracold gas. *Phys. Rev. Lett.* **2004**, *93*, 063001. [[CrossRef](#)] [[PubMed](#)]
- Urban, E.; Johnson, T.A.; Henage, T.; Isenhower, L.; Yavuz, D.; Walker, T.; Saffman, M. Observation of Rydberg blockade between two atoms. *Nat. Phys.* **2009**, *5*, 110–114. [[CrossRef](#)]
- Gaëtan, A.; Miroshnychenko, Y.; Wilk, T.; Chotia, A.; Viteau, M.; Comparat, D.; Pillet, P.; Browaeys, A.; Grangier, P. Observation of collective excitation of two individual atoms in the Rydberg blockade regime. *Nat. Phys.* **2009**, *5*, 115–118. [[CrossRef](#)]
- Scully, M.; Fry, E.; Ooi, C.; Wodkiewicz, K. Directed Spontaneous Emission from an Extended Ensemble of  $N$  Atoms: Timing Is Everything. *Phys. Rev. Lett.* **2006**, *96*, 010501. [[CrossRef](#)]
- Svidzinsky, A.A.; Chang, J.T.; Scully, M.O. Dynamical Evolution of Correlated Spontaneous Emission of a Single Photon from a Uniformly Excited Cloud of  $N$  Atoms. *Phys. Rev. Lett.* **2008**, *100*, 160504. [[CrossRef](#)]
- Svidzinsky, A.A.; Chang, J.T.; Scully, M.O. Cooperative spontaneous emission of  $N$  atoms: Many-body eigenstates, the effect of virtual Lamb shift processes, and analogy with radiation of  $N$  classical oscillators. *Phys. Rev. A* **2010**, *81*, 053821. [[CrossRef](#)]
- Courteille, P.W.; Bux, S.; Lucioni, E.; Lauber, K.; Bienaimé, T.; Kaiser, R.; Piovela, N. Modification of radiation pressure due to cooperative scattering of light. *Eur. Phys. J. D* **2010**, *58*, 69–73. [[CrossRef](#)]
- Bienaimé, T.; Bux, S.; Lucioni, E.; Courteille, P.; Piovela, N.; Kaiser, R. Observation of a Cooperative Radiation Force in the Presence of Disorder. *Phys. Rev. Lett.* **2010**, *104*, 183602. [[CrossRef](#)]
- Bienaimé, T.; Bachelard, R.; Piovela, N.; Kaiser, R. Cooperativity in light scattering by cold atoms. *Fortschritte Der Phys.* **2013**, *61*, 377–392. [[CrossRef](#)]
- Bienaimé, T.; Piovela, N.; Kaiser, R. Controlled Dicke Subradiance from a Large Cloud of Two-Level Systems. *Phys. Rev. Lett.* **2012**, *108*, 123602. [[CrossRef](#)] [[PubMed](#)]
- Guerin, W.; Araújo, M.O.; Kaiser, R. Subradiance in a Large Cloud of Cold Atoms. *Phys. Rev. Lett.* **2016**, *116*, 083601. [[CrossRef](#)]
- Scully, M.O. Single photon subradiance: Quantum control of spontaneous emission and ultrafast readout. *Phys. Rev. Lett.* **2015**, *115*, 243602. [[CrossRef](#)] [[PubMed](#)]

26. Svidzinsky, A.A.; Zhang, X.; Scully, M.O. Quantum versus semiclassical description of light interaction with atomic ensembles: Revision of the Maxwell-Bloch equations and single-photon superradiance. *Phys. Rev. A* **2015**, *92*, 013801. [[CrossRef](#)]
27. Cai, H.; Wang, D.W.; Svidzinsky, A.A.; Zhu, S.Y.; Scully, M.O. Symmetry-protected single-photon subradiance. *Phys. Rev. A* **2016**, *93*, 053804. [[CrossRef](#)]
28. Gegg, M.; Carmele, A.; Knorr, A.; Richter, M. Superradiant to subradiant phase transition in the open system Dicke model: Dark state cascades. *New J. Phys.* **2018**, *20*, 013006. [[CrossRef](#)]
29. Tóth, G.; Knapp, C.; Gühne, O.; Briegel, H.J. Optimal spin squeezing inequalities detect bound entanglement in spin models. *Phys. Rev. Lett.* **2007**, *99*, 250405. [[CrossRef](#)]
30. Akkermans, E.; Gero, A.; Kaiser, R. Photon localization and Dicke superradiance in atomic gases. *Phys. Rev. Lett.* **2008**, *101*, 103602. [[CrossRef](#)]
31. Bellando, L.; Gero, A.; Akkermans, E.; Kaiser, R. Cooperative effects and disorder: A scaling analysis of the spectrum of the effective atomic Hamiltonian. *Phys. Rev. A* **2014**, *90*, 063822. [[CrossRef](#)]
32. Ellinger, K.; Cooper, J.; Zoller, P. Light-pressure force in N-atom systems. *Phys. Rev. A* **1994**, *49*, 3909. [[CrossRef](#)] [[PubMed](#)]
33. Bienaimé, T.; Petruzzo, M.; Bigerni, D.; Piovella, N.; Kaiser, R. Atom and photon measurement in cooperative scattering by cold atoms. *J. Mod. Opt.* **2011**, *58*, 1942–1950. [[CrossRef](#)]
34. Scully, M.O.; Svidzinsky, A.A. The Lamb Shift—Yesterday, Today, and Tomorrow. *Science* **2010**, *328*, 1239–1241. [[CrossRef](#)] [[PubMed](#)]
35. Kitagawa, M.; Ueda, M. Squeezed spin states. *Phys. Rev. A* **1993**, *47*, 5138–5143. [[CrossRef](#)] [[PubMed](#)]

**Disclaimer/Publisher's Note:** The statements, opinions and data contained in all publications are solely those of the individual author(s) and contributor(s) and not of MDPI and/or the editor(s). MDPI and/or the editor(s) disclaim responsibility for any injury to people or property resulting from any ideas, methods, instructions or products referred to in the content.